HHS Public Access

Author manuscript

Sci Total Environ. Author manuscript; available in PMC 2020 March 24.

Published in final edited form as:

Sci Total Environ. 2019 March 25; 658: 1549–1558. doi:10.1016/j.scitotenv.2018.12.159.

Effectiveness of vegetation and sound wall-vegetation combination barriers on pollution dispersion from freeways under early morning conditions

Dilhara Ranasinghe[a,i], **Eon S. Lee**[b,ii], **Yifang Zhu**[b], **Isis Frausto-Vicencio**[a], **Wonsik Choi**[a,iii], **Wu Sun**[a], **Steve Mara**[c], **Ulrike Seibt**[a], **Suzanne E. Paulson**[a,*]

[a]University of California, Los Angeles, Department of Atmospheric and Oceanic Sciences, 405 Hilgard Ave., Los Angeles, CA 90095, USA.

[b]University of California, Los Angeles, Department of Environmental Health Sciences, 650 Charles Young Dr., Los Angeles, CA 90095, USA

[c]California Air Resources Board, Research Division, Sacramento, CA 95812, USA

Abstract

Pollutants in tailpipe emissions can be highly elevated around roadways, and in early mornings the pollution plume can extend hundreds of meters into surrounding neighborhoods. Solid sound walls and vegetation barriers are commonly used to mitigate noise, but they also help mitigate near-road air pollution. Here we assess the effectiveness of barriers consisting of vegetation only and of a combination of vegetation and a solid sound wall (combination barrier) in reducing pollution concentrations downwind of roads, under stable atmospheric stability and calm to light wind conditions. Because there was no practical (no barrier) control site in the area, we primarily compare the two barrier types to each other and explore the importance of atmospheric conditions. Using measurements collected with a mobile platform, we develop concentration decay profiles of ultrafine and fine particles, oxides of nitrogen (NO and NO_2) and carbon monoxide downwind of a freeway in California with different barrier configurations and meteorological conditions. Diurnally averaged data collected with passive samplers indicate that pollution from morning rush hour has about equal impact as the entire remainder of the day, because of differences in atmospheric dispersion as the day progresses. Under calm and stable atmospheric conditions (wind speed < 0.6 m/s); a vegetation-only barrier was more effective than a combination barrier with a total height that was somewhat lower than the vegetation-only barrier, by 10–24 % in the first 160 m downwind. Under light winds (above ~ 0.6 but below 3 m/s) and stable conditions, the combination barrier was more effective the vegetation barrier alone, by 6–33%, in the first 160 m from the barrier. The average particle size downwind of the vegetation-only barrier was larger than downwind of the combination barrier, indicating that particle deposition plays an important role in the reductions observed downwind of vegetation. Our results are consistent with the notion that at low wind speeds, vegetation acts as an effective barrier. Overall, adding vegetation alone or to an

*Corresponding author. paulson@atmos.ucla.edu. Tel.: 310 206 4442.

[i]Present address: California Department of Pesticide Regulation, 1001 I Street, Sacramento, CA 95814

[ii]Present address: California Air Resources Board Monitoring & Laboratory Division, 9480 Telstar Ave., El Monte, CA 91731, USA

[iii]Present address: Department of Environmental Atmospheric Sciences, Pukyong National University, 45 Yongso-ro, Nam-gu, Busan, Republic of Korea

existing solid barrier results in lower downwind pollution concentrations, especially under low wind speeds when concentrations can be high.

1. INTRODUCTION

Roadway vehicles emit a suite of air pollutants including coarse ($PM_{10–2.5}$; particle diameters between 2.5 – 10 μm), fine ($PM_{2.5}$; particle diameter less than 2.5 μm) and especially ultrafine (UFP/ $PM_{0.1}$; particle diameter less than 0.1 μm) particles; carbon monoxide (CO); carbon dioxide (CO_2); nitrogen oxides (NO_x); black carbon (BC); polycyclic aromatic hydrocarbons (PAHs) and volatile organic compounds (VOCs). Air quality studies conducted near heavily trafficked roads show that many of these pollutant concentrations are elevated on and near roads. The degree of pollutant elevation depends on the source strength in comparison to the urban background, however, such that some pollutants are only slightly elevated ($PM_{2.5}$, $PM_{10,}$ CO_2), while others are highly elevated (UFP, NO_x) (Karner et al., 2010 & references therein).

A growing body of epidemiological studies show that exposure to elevated levels of roadway pollutants are associated with increases in a variety of adverse health outcomes (Landrigan et al., 2017). An estimated 30–45% of people in large North American cites live within zones highly impacted by traffic emissions, covering up to 300–500 m from a highway or a major road (HEI, 2010). Recognizing the potential for negative impacts from placing sensitive land uses such as residences, schools, day care centers, playgrounds and medical facilities near busy roads, new laws and mitigation strategies have been implemented to reduce the exposure of near-road communities to pollutants emitted by vehicles. Some of the widely considered mitigation strategies for exposure reduction are the optimization of noise barriers, roadside vegetation, road surface cleaning, dust binders, and dynamic traffic management using air quality forecasts.

Physical barriers affect pollutant concentrations by increasing turbulence and initial mixing of the emitted pollutants (Hölscher et al. 1993). Roadside solid sound walls (SW) force pollutants to move up and over the barrier, creating the effect of an elevated source and enhancing vertical dispersion of the plume. The dispersion is further enhanced by a highly turbulent shear zone characterized by low velocities and a recirculation cavity created on the lee side of the barrier. These effects contribute to a well-mixed zone with lower pollutant concentrations downwind behind the barrier (Bowker et al. 2007).

Vegetation barriers have potential to alter flow as well, but with several differences. Vegetation imposes a drag on the air moving through the leaves and branches. This flow obstruction causes some air to move up and around the canopy, increasing vertical mixing and in turn reducing pollution concentrations downwind of the barrier. Vegetation can also remove some gaseous pollutants by absorption and particulate matter by deposition (Abhijith et al., 2017 and references therein). The deposition of the smallest particles is controlled by Brownian diffusion, while interception and inertial impaction determine the deposition of larger particles (Petroff et al. 2008). On the other hand, the imposed drag on the airflow creates a windbreak effect behind the vegetation barrier, characterized by lower wind speeds and lower turbulence in the wake of the canopy (Wang et al., 2001). This

windbreak effect decreases both dispersion and the rate at which traffic-related pollutants can be advectively transported away, potentially increasing the pollutant concentrations downwind of the vegetative barrier.

While general features of pollutant concentrations downwind of barriers are emerging, concentrations downwind of specific barriers can vary widely depending on many factors. For solid sound walls, the dominant features include the physical characteristics of the barrier such as the height, length, distance from road, number of barriers and their orientation with respect to the wind (Hagler et al., 2011; Heist et al., 2009), meteorological conditions such as wind speed, wind direction and atmospheric stability (Baldauf et al., 2008; Finn et al., 2010), traffic activity such as vehicle volume, speed and fleet mix (Baldauf et al., 2008), and configuration of the road such as the elevation/depression relative to the terrain (Heist et al., 2009) and surrounding structures/vegetation (Bowker et al., 2007). The impact of vegetation barriers on pollution dispersion can depend on several additional variables, including density of the vegetation, seasonal growth patterns, leaf type (Fujii et al., 2008), leaf area index (LAI)/leaf area density (LAD)/optical porosity (Steffens et al., 2012; Ghasemian et al., 2017), tree canopy type. While partly overlapping with the optical porosity parameter, the thickness of the tree stand can also be a factor (Baldauf et al., 2017).

In open street environments, solid sound walls can reduce the UFP concentrations by up to about 50% compared to open road values within 15–50 m on the lee side of a sound wall (Bowker et al., 2007; Baldauf et al., 2008; Heist et al., 2009; Ning et al., 2010; Finn et al., 2010). Understanding of the effectiveness of combination barriers (sound walls together with vegetation barriers) is very limited (Bowker et al., 2007; Baldauf et al., 2008). One field study showed that a combination barrier augmented the reduction of pollutants compared to sound wall-only values (Baldauf et al., 2008), but the authors acknowledged that the proximity of the measurement transects to the edge of the barrier and wind directions during the study might have influenced their results. The impact of vegetation barriers alone on pollution dispersion is also an open question; studies of this barrier configuration have produced inconsistent findings. While some field work (Hagler et al., 2012; Tong et al., 2015; Morakinyo et al., 2016) showed high variability in the effectiveness of vegetation barriers alone, other studies found reductions of UFP (Steffens et al., 2012; Al-Dabbous et al., 2014; Lin et al., 2016; Lee et al., 2018), $PM_{2.5}$ (Chen et al, 2016), PM_{10} (Chen et al.,2015), BC (Brantley et al., 2014), CO (Lin et al.,2016) and NO_2 (Fantozzi et al. 2015a) behind vegetation barriers. Furthermore, vegetation varies widely with location.

Atmospheric stability can have a large impact on the spatial extent of freeway pollution plumes (Finn et al., 2010; Hu et al., 2009; Choi et al., 2012; Choi et al., 2014). Field studies have shown that in pre-sunrise stable boundary layers, freeway pollution plume can extent up to 2.5 km. Even though the traffic emissions are low overnight and in the early morning, pollution concentrations can be higher than daytime due to the near-ground trapping caused by nocturnal stable atmospheric conditions (Hu et al., 2009; Choi et al., 2012; Choi et al., 2014).

Here we attempt to develop a better understanding of the effectiveness of vegetation usually found in the semi-arid climate of California in reducing the pollution concentrations

downwind of roads under different meteorological conditions. We present results from an extensive field measurement campaign to investigate the pollution reduction efficiency of vegetation and sound wall-vegetation combination barriers. Data from mobile and stationary measurements were collected at a site in Santa Monica California during the early morning. We use 1-second time resolution ultrafine particle data to examine the effects of the barriers under different meteorological conditions, and on the mechanisms leading to particle reductions downwind of the vegetative and combination barriers. Lower time/spatial resolution gas concentration profiles are also presented. Companion measurements made in Sacramento, California during daytime will be discussed in a forthcoming paper (Ranasinghe et al., 2019).

2. MEASUREMENTS

Most mobile measurements were conducted using the ARB mobile monitoring platform (ARB-MMP), an electric sub-SUV fitted with a suite of instruments that measure several particulate and gas phase pollutants (Table 1). The ARB-MMP inlet design and calibration procedures are provided elsewhere (Hu et al., 2009; Choi et al., 2012) and thus are described only briefly here. Particle and gas instruments were calibrated before each measurement season. Flow checks and zero checks of instruments were performed at the start and end of each measurement session. For the summer measurement session, a zero-emission electric vehicle equipped with a DiSCmini (Testo) and a GPS unit (Qstar XT) was used as the MMP. At each site, mobile measurements were performed on two transects with different barrier configurations, selected to be close to perpendicular to a heavily trafficked freeway (Fig. 1). The MMP was driven 12–14 runs (a run is a pass of the MMP along the full length of the sampling route) on the downwind side on each transect and at least three runs on the upwind side. The downwind runs were conducted in six sets of 4–5 runs, completed by alternating between the two transects, with upwind runs at both locations between downwind measurements sets. While completing each upwind run, the MMP was stopped to collect stationary measurements for 2–5 min at an upwind location 20–25 m from the edge of the freeway. It is important to emphasize that the same instrument (a DiSCmini) was used on all transects.

The field performance of the DiSCmini is discussed in detail in Choi et al. (2016). Briefly, we have found the DiSCminis to agree within about ± 10 % of a condensation particle counter (CPC) within the range of the CPC, and to agree perfectly with the average size of the scanning mobility particle sizer (Choi et al., 2016). Individual DiSCminis have slightly different slopes with respect to each other and the CPC due to the individual instrument differences and /or the inlet tubing. The slopes were not observed to drift over periods of many months, with $R^2 \approx 0.9$ (Choi et al., 2016 supplementary).

A series of passive NO/NO_x samplers (Ogawa Inc., Pompano Beach, FL) measured multi-day average profiles at 6 – 8 points along each transect. The passive NO/NOx samplers were attached 2–3 m above ground level to available structures (e.g., trees, lampposts, and street signs) for the duration of each measurement campaign. At the end of the measurement campaign, they were recovered, sealed and sent to RTI International (Research Triangle,

NC) for analysis, including corrections for response dependence on relative humidity and temperature.

NO_2 concentrations were determined from the difference of the time-averaged NO and NO_x measurements. Wind speed and direction was measured with a sonic anemometer (10 Hz CSAT3, Campbell Sci. Inc., 21 Hz WindMaster, Gill Instruments Ltd.) that was installed on a rooftop close to measurement transects (Fig.1).

Average heights and optical porosities were estimated for vegetation within ± 100 m of the measurement transects as discussed in SI1 and shown in Figs. SI1 and 2. Optical porosity of the vegetation is defined as the fraction of pore spaces and gaps in the total area of the tree crown profile. High optical porosity corresponds to low density vegetation and/or large amounts of gaps between trees. The optical porosity of the vegetation barriers was estimated by measuring the optical porosity of each tree crown according to a US Forest Service field guide for vegetation characterization (USFS, 2011). The horizontal dimensions of the trees and their heights with respect to the highway road surface were measured in Google Earth Pro. The effective optical porosity of vegetation at a site was calculated by rescaling the mean optical porosity of the site to maximum height of vegetation at either site (SI 1).

The I-10 freeway had an east-west orientation at the measurement sites in Santa Monica, CA (34° 1’35.97”N/ 118°27’33.66”W). In the early-mornings, the prevailing winds were mostly northerly, and the sound wall of interest was on the south side of the freeway. Downwind mobile measurements were conducted in the mornings (05:00–07:30) on Dorchester Ave. where a combination (sound wall and vegetation) barrier (CB) was present, and on Granville Ave. where a vegetation-only barrier (VB) was present (Fig. 1). The transects were approximately 840 m long. Upwind measurements were conducted on Dorchester Ave. and Granville Ave., on the north side of the freeway. Measurements were performed in late summer/early fall 2015 and winter 2016 (Table 2). Only UFP measurements were collected during the late summer session and they were grouped with early fall measurements (summer/fall) because the meteorology during both periods was similar. Relative to ground level, the I-10 freeway is elevated by approximately 6 m on both sites. The height of the sound wall at the CB is approximately 4 m. The vegetation at the VB site was considerably denser (lower optical porosity) and somewhat taller than the vegetation at the CB site. The mean height and the effective optical porosity of vegetation was 8 m and 0.53, 6 m and 0.79 at the VB and CB sites, respectively (Table SI2). The along-wind-direction thickness of the vegetation stands varied from 5–25 m, and the approximate mean thickness was 15 and 12 m at the VB and CB sites, respectively (Fig. SI2). Except for several cypress trees at VB site and a pine at CB site, all species are evergreen broadleaf trees; none drop their leaves in winter.

3. DATA ANALYSIS METHODOLOGY

3.1 Concentration plots

Deriving accurate concentration profiles from a series of concentration measurements collected on different days and under slightly different conditions requires several steps. Without careful consideration, it is easy to over- or under-weigh some points and/or runs,

allow contamination by high-emitting vehicles on the road where sampling was performed to obscure the target source freeway, or include data for runs when the winds were not perpendicular to the freeway. Here we describe the approaches used to handle these limitations. Many of the approaches used here were developed in Ranasinghe et al. (2016) and Choi et al. (2012, 2013) and are described only briefly here.

First, data from different instruments on the MMP were synchronized to account for any differences in response times of instruments and inlet configurations, using the time-lag correlation method described in detail in Choi et al. (2012). Next, the contribution from high-emitting vehicles (HEV) encountered along the sampling route was removed by adapting the method developed in Choi et al. (2013) to identify HEV-related spikes, as described in detail in the SI. This method uses an iterative statistical approach to establish a site- and session-specific baseline threshold to determine events caused by HEVs, using a specified smoothing time window (60 s) to estimate the baseline. Close to the freeway, it is more difficult to distinguish the freeway plume from local traffic emissions. To address this, the threshold value was increased for distances close to the freeway (detailed in SI 2). Very close to the freeway where traffic on the transect was light, all data points were retained, and short-lived spikes observed in the time series were manually removed by identifying HEV-related incidents using traffic video from the MMP. This method successfully removes the narrow HEV-related spikes while retaining the wider freeway-related spikes.

The effect of barriers on pollution dispersion downwind of freeways has been shown to be strongly dependent on the wind direction (Finn et al., 2010, Steffens et al., 2012). We used the meteorological data collected at an upwind location to partition all concentration data according to wind direction. The concentration data were divided into near-perpendicular and near-parallel data sets, defined as wind coming from ± 45° from perpendicular or ± 45° from parallel to the freeway, respectively. Next, all concentration data sets were normalized by the freeway traffic flow at each site as described below (Section 3.2). As the concentration measurement at a particular time and distance from the freeway is influenced by the emissions and the wind direction from several minutes earlier, we introduced a 10 min lag in traffic flow normalization and wind direction selection, based on the average travel time of pollutants from the source to the transects. At each data point, the average traffic flow and wind direction from 10 min earlier was calculated and used for the traffic flow normalization and wind filter.

Next, we used the line reference system developed by Ranasinghe et al. (2016) to provide a framework to organize the data and produce concentration maps at specific spatial resolutions. With this procedure, the GPS data for each run (one pass of the MMP along the sampling route) was used to assign each concentration data point to the closest line reference point along the street. Then for each session, all data values assigned to a reference point were averaged, and the standard deviation of the mean calculated. There is a higher data density at the ends of the transects because the MMP was slowed to turn around, and the concentration changes most rapidly near the freeway. The GPS location data had 2.5 m accuracy with wide area augmentation system (WAAS). To exploit this spatial resolution of location data and the higher concentration data density at the start of the transect, we used a 10 m spatial resolution in the first 30 m and 20 m spatial resolution thereafter. The number

of data points averaged at a line reference point was 31 ± 17. For $PM_{2.5}$ and PM_{10} profiles, we used a 40 m spatial resolution because data collected using the OPS had lower time resolution (5 s, Table 1).

From day to day, average pollution concentrations vary by a factor of two or more, due to meteorological phenomena such as mixing height, turbulence intensity and atmospheric stability. These variations in the urban background must be accounted for prior to averaging data from different sessions and days to avoid over/under weighting. In this study, the upwind stationary and mobile measurements were made at 15 m and 20–150 m from the edge of the freeway, respectively. However, data from these measurements were not used for several reasons: the upwind measurements were likely too close to freeway; Choi et al. (2012) showed some influence from the freeway up to 500 m during early mornings, and the sites were influenced by variable winds making the upwind site intermittently downwind. This resulted in a small upwind data set after the wind filters were used to isolate ‘true upwind’ periods and limited our ability to extract a representative urban background from that data set.

Given the lack of a representative urban background, the daily maximum was used to normalize the data. This allowed us to retain the differences between the profiles of the two transects from each day and allowed averaging over all measurement days of a season without over/underweighting. The daily maximum concentration of transects was obtained from daily average concentration profiles made from HEV-removed, wind filtered data averaged at line reference points. Then the daily average concentration profiles of both transects were normalized by dividing all values by the daily maximum concentration. A sensitivity test was preformed to investigate the effect of the normalization procedure on UFP concentration profiles and relative reduction percentages, by comparing a daily maximum and a daily minimum normalization (SI 9). Use of either the daily maximum or the minimum resulted in similar session average concentration plots, indicating a low sensitivity of the daily maximum normalization on the barrier comparison results.

Each day had a different number of data points corresponding to the percentage of time each transect was downwind during the measurement period. Moreover, as consistent winds give higher quality data and a clearer freeway plume decay pattern, we used a weighting factor based on the mean percentage of time transects were downwind on each day. If the mean percentage of time the transects was downwind was below 25%, that day was excluded from the average.

3.2 Traffic flow variations

To correct for time and day-dependent variations in traffic, 5 min resolution traffic data was retrieved from the Caltrans Performance Measurement System (PeMS). We chose the closest main-line sensor on the freeway for each measurement transect and each traffic flow direction, provided that the sensor had > 99% observation rate. All main-line traffic sensors were within 2 km of the transects. When there were on/off-ramps between a selected main-line sensor and the target measurement transect, either measured or historic traffic flow rates from on-ramp/off-ramp sensors were used to estimate the traffic flow at each transect. Traffic data had 5-min time resolution.

Figure SI5 shows 30 min means and standard deviations of the means of the traffic flow in both directions at each measurement transect. The day-to-day variation in the traffic flows in was small, but average flows were slightly different at the two transects; the freeway traffic flow near Granville Ave. was 2.5% and 4.9% higher than the freeway traffic flow near Dorchester Ave. in the fall and winter seasons, respectively.

4. RESULTS AND DISCUSSION

4.1 Combination barrier vs. vegetation barrier

Figs. 2a and b shows the average decay profiles for traffic-normalized ultrafine particle number concentration [UFP] under perpendicular wind conditions, and early morning stable atmospheric conditions. In agreement with the earlier studies (Hu et al., 2009; Choi et al., 2012; Choi et al., 2014), [UFP] gradually decreases throughout the full length of the transect (840 m) in both sessions. The [UFP] reduction behind the barriers showed different trends in the summer/fall and winter measurement sessions. Under perpendicular wind conditions, in the summer/fall session, the vegetation-only barrier was more effective in reducing downwind [UFP] than the combination barrier (Fig. 2a), while in the winter session, the combination barrier was more effective than the vegetation-only barrier (Fig. 2b). In the summer/fall season, the traffic-normalized [UFP] downwind of the vegetation-only barrier during perpendicular winds was 24% lower than the combination barrier (Fig. 2a), averaged over the entire transect (800 m). Averaged over the first 160 m (~ 525 ft.), this difference was 27%. For the winter season, the traffic-normalized [UFP] downwind of the combination barrier during perpendicular winds was 6% lower than the vegetation-only barrier (Fig. 2b) averaged over the entire transect. Averaged over the first 160 m from the edge of the freeway, this difference was 16%.

The surface meteorology in the summer/fall vs. winter sessions was different in several respects that likely contributed to the observed differences in pollution plume decay downwind of the freeway. The average wind speed in the summer/fall session was 0.3 ± 0.1 m/s, while in the winter session it was 1.1 ± 0.6 m/s; the wind speed dependence of the pollution reduction is discussed in section 4.2. Also, the wind direction was more variable in the summer/fall session than in winter; the average percent time transects were downwind of the freeway (as defined in section 3.1) was 55 ± 22% in the summer/fall session and 69 ± 21% in the winter session. When variable winds cause intermittent switching of the side that is downwind, the (mostly) upwind pollution levels tend to increase and (mostly) downwind pollutions levels tend to decrease, affecting the downwind concentration decay profile.

The pollution profiles are less influenced by the freeway pollution plume under parallel/near-parallel wind conditions and likely to be more influenced by local sources. Compared to the perpendicular wind case, [UFP] decay profiles under parallel wind conditions (Fig. SI11) showed only small reductions along each transect. After a limited initial decay of [UFP] in first 60–80 m behind the vegetation barrier, there was no significant difference in the concentrations behind the different barriers.

$PM_{2.5}$ and PM_{10} mass concentration ([$PM_{2.5}$] and [PM_{10}]) data were not available for the summer or fall seasons (above). In winter, under perpendicular wind conditions, the traffic

normalized downwind [$PM_{2.5}$] (Fig. 2c) and [PM_{10}] (Fig. 2d) showed a small, gradual decay with increasing distance in the first 200 m from the freeway, and the particle concentrations behind the combination barrier were lower compared to the vegetation-only barrier. This gradual decay is due to the fact that the freeway causes only slight increases in these pollutants above their backgrounds (Karner et al., 2010; Choi et al., 2014). The concentration difference that extends along the full length of the transect indicates the likely contribution from an additional area-wide source of $PM_{2.5}$ and PM_{10}. However, the barrier effect on $PM_{2.5}$ and PM_{10} concentrations is similar to that on UFP; the combination barrier was more effective in reducing fine/coarse particulate matter than the vegetation-only barrier under winter meteorological conditions.

Continuous stationary measurements of particulate matter conducted at a site in Encino, CA, a site with a similar barrier configuration (CB and VB); found the same pattern of pollution reduction. For both [UFP] and [PM2.5], a combination barrier was more effective reducing downwind pollution concentrations under perpendicular wind conditions (Lee et al. 2018). The Lee et al. (2018) analysis did not distinguish between day and nighttime data. Under perpendicular winds, the average wind speed in that study was 1.1 ± 0.75 m/s. The combination barrier had higher, thicker and more dense (lower optical porosity) vegetation compared to the vegetation only site, opposite of the characteristics of the Santa Monica site that had a combination barrier with shorter, thinner and less dense (higher optical porosity) vegetation compared to the vegetation only site. This indicates that regardless of the atmospheric stability and differences site/barrier characteristics, under moderate wind speeds, combination barriers are more effective in reducing downwind UFP and PM2.5 concentrations, than a vegetation barrier alone.

Earlier studies have shown reductions in UFP by vegetation stands either comparable or lower in height (3.4 −8 m) and thinner (2 −4.5 m) compared to the height (8 m) and width (~15m) of the vegetation-only barrier in this study (Hagler et al., 2012; Al-Dabbous et al., 2014; Lin et al., 2016).

Decay trends of several gas phase pollutants were generally similar to particulate matter pollutants trends. Fig. 3 shows the average traffic-normalized concentration profiles of NO (Fig. 3a, b), NO_2 (Fig. 3c, d) and CO (Fig. 3e, f) under perpendicular winds. For all three gas phase pollutants, the reduction downwind of the combination barrier was smaller than the vegetation-only barrier in the fall season (Fig. 3a, c and e); and larger than the vegetation-only barrier in winter (Fig. 3b, d and f). In the fall, under low wind speeds, a gradual decay was observed along the entire transect. In the winter, under higher wind speeds, a relatively steeper decay was observed in the first 100 m from the freeway, followed by a gradual decay along the rest of the transect.

NO/NO_x passive samplers reported NO_x concentrations similar to the MMP measurements. The concentrations from passive samplers (entire sampling periods, 24 h/day) showed no significant difference between the two barrier configurations in either the fall (Fig. SI7) or winter (Fig. SI8) sessions. There was a general concentration decay going away from the freeway and the concentrations were very slightly higher on the north (nominally upwind) side of the freeway (negative distances in Figs. SI7 and SI8). This can be explained as

follows. The Santa Monica site commonly receives a weak land breeze from the north during the night and early morning, but experience a persistent sea breeze most days, from mid-morning (9–11 am depending on season) into evening. Traffic on the freeway is minimal at night, so the morning downwind, south side of the freeway only receives pollution during morning rush hours. This brief period results in concentrations that are nearly the same as the entire remainder of the day into evening, including the afternoon rush hour.

4.2 Wind speed dependence of [UFP] pollution reduction

The pollution reduction behind vegetation barriers is attributed to increases in vertical mixing, and removal of some pollutants via uptake and deposition. The windbreak effect, which slows air flow due to the drag imposed on air moving through the porous vegetation barriers has the potential to increase pollution concentrations downwind. Since the porosity, drag force and particle deposition are wind speed dependent, the pollution concentration reduction by vegetation barriers is expected to be particle size and wind speed dependent. The relative [UFP] reduction percentage of a combination barrier, in comparison with the vegetation-only barrier was calculated as follows:

$$Relative\ reduction = \frac{VEG - CB}{\max(VEG, CB)} \times 100\% \quad \text{(Eq. 1)}$$

Where CB is the [UFP] behind the combination barrier, VEG is the [UFP] behind the vegetation-only barrier. The relative reduction averaged over the first 160 m from the edge of the freeway plotted against wind speed averaged over each measurement day is shown in Fig. 4.

Figure 4a shows that the relative reduction in [UFP] is strongly dependent on wind speed. The vegetation-only barrier is more effective in reducing [UFP] than the combination barrier at very low wind speeds (< 0.6 m/s), indicated by negative relative reduction values, and less effective than the combination barrier at higher wind speeds. Higher wind speeds can increase vegetation porosity, lowering drag force within the vegetation canopy and vertical dispersion, but the difference in vegetation porosity and drag force over the observed wind speed range is expected be small (Kent et al., 2017); larger differences are expected for higher wind speeds (Gromke et al., 2008; Tiwary et al., 2006; Janhäll et al., 2015). At higher wind speeds the residence time of the air mass inside the canopy decreases, decreasing time for absorption/depositional removal of pollutants. This dynamic depositional removal efficiency of particles may be the main contributor to the observed wind dependence of the relative reduction; depositional removal of UFP by vegetation is discussed further in section 4.4.

The observed wind speed dependence of the effectiveness of vegetation barriers in removing UFP (Fig. 4a) agrees with a previously reported study that used a comprehensive turbulent aerosol dynamics gas chemistry model for vegetation barriers (Steffens et al., 2012) and a wind tunnel study of vegetation branches and leaves (Lin and Khlystov, 2012). Lin and Khlystov (2012) reported that the UFP removal efficiency decreased with increasing particle size, increasing wind speed and decreasing packing density (volume fraction occupied by

the vegetation). The sensitivity to wind speed of removal efficiency reported by Steffens et al. (2012) for small particle sizes (< 50 nm) was similar to that found in Lin and Khlystov (2012), but the results diverged for larger particle sizes. Steffens et al. (2012) reported that for particles larger than 50 nm, the UFP removal efficiency increased with increasing wind speed.

An investigation of the relation between atmospheric stability (Monin-Obukov length, L) and the relative reduction in [UFP] is presented in Fig. 4b. Although all measurement days had very stable atmospheric conditions (small positive L), L was somewhat variable. However, no clear relation was found between the relative reduction and L. In conclusion, relative reduction has a clearer relationship with wind speed than to the atmospheric stability parameter L. The wind speed-dependence of the relative reduction of pollutants such at $PM_{2.5}$, NO, NO_2 was generally similar to that of UFP, while some pollutants such as PM_{10} and CO showed different patterns (SI 6).

4.4 Removal of Ultrafine particles by deposition

Figure 5 shows the mean size of UFP downwind of the vegetation-only and combination barriers at the Santa Monica site in the two seasons. Even though the pollution reduction patterns behind barriers showed a seasonal difference (Fig. 2a and b), the mean size of UFP was larger downwind of the vegetation-only barrier in both seasons. While the differences are modest, the measurements were collected with the same instrument, and in a paired two-tail t-test the difference in the first 160 m was statistically significant ($p < 0.01$) in both seasons.

Roadside vegetation barriers force one part of the freeway plume to move up and over the barrier, while the remainder flows through the porous barrier. A fraction of the particles in the flow passing through the vegetation can be removed by deposition to the canopy. The contribution of deposition to particle reduction by vegetation barriers near roadways is a complex function of the characteristics of the vegetation barrier, the particles and meteorological parameters. Deposition is a strong function of particle size (Lin et al., 2011), thus particle size provides some insight into the importance of deposition in reducing particle concentrations downwind of vegetation barriers. For UFP, diffusion is the dominant mechanism of deposition. Smaller particles have higher deposition velocities and are more efficiently removed (Fujii et al., 2008, Lin & Khlystov, 2012), thus disposition increases the mean size of the particles downwind of a vegetation barrier.

The increase in vertical mixing created by a solid barrier is larger than that of a vegetation barrier (Ghasemian et al., 2017). The background air that is mixed with the freeway plume has larger particles than the freeway plume coming from the source; Choi and Paulson (2016) showed an upwind background with a peak at ~50 nm and very close to freeway peak at ~10 nm (although mean diameters were larger). As a result, a barrier that creates more vertical mixing should increase the average particle size downwind -- thus, dispersion alone should produce larger particle sizes downwind of a solid or combination barrier than it would downwind of a vegetation barrier. We observe the opposite trend in particle size (Fig. 5); particles were larger downwind of the denser vegetation-only barrier under the low and

moderate wind speeds in our study. This is evidence for a strong contribution of deposition to reducing UFP downwind of vegetation barriers, especially when wind speeds are low.

The seasonal difference in the mean size of particles (Fig. 5) further supports a large role for deposition. The difference in the particle size downwind of the two barriers in the first 160 m is much larger in the low windspeed summer-fall season than in winter. The depositional removal of particles has been shown to be more efficient at lower wind speeds (Fujii et al., 2008, Lin et al., 2011).

The windbreak effect of vegetation barriers reduces the flow velocity inside and downwind of the canopy. This increases the residence time of particles in the flow through the vegetation barrier, which also allows more time for coagulation, which would increase the mean size of the particles downwind. However, the timescale for deposition is approximately an order of magnitude faster than for coagulation, and therefore coagulation is estimated to be a minor contributor at the neighborhood scale (Choi and Paulson, 2016).

5. CONCLUSIONS

High-resolution profiles developed from mobile measurements show that for roughly perpendicular winds, elevated ultrafine particle concentrations at the edge of the freeway decay within about 500 m or more during calm conditions in the early morning, consistent with earlier studies. This study indicates that for the optical porosities reported here, both vegetation and combination barriers are effective near-road air pollution mitigation strategies that can be used by urban planners and policy makers. For perpendicular winds, adding vegetation alone or to an existing solid barrier results in lower downwind pollution concentrations, especially under low wind speeds when concentrations are higher. The largest benefit was observed closer to the barrier (Table 3). In the calm early mornings, the taller and rather dense vegetation-only barrier was more effective than the combination barrier at very low wind speeds (< 0.6 m/s), but at higher wind speeds the combination barrier was more effective. Under parallel wind conditions, when the freeway plume has a much smaller impact on pollutant concentrations in adjacent communities, pollution was elevated only slightly or not at all near the edge of the freeway, thus barrier design is of little consequence.

The pollution reduction by vegetation barriers is strongly dependent on wind speed and the density/optical porosity of the vegetation. The choice of barrier can also be constrained by factors such as the cost, resources available for vegetation growth/maintenance. Further research into the impacts of these factors is desirable.

Supplementary Material

Refer to Web version on PubMed Central for supplementary material.

Acknowledgements

The authors are grateful for the research support provided by the California Air Resources Board (CARB), Contract No. 13-306. The views and opinions expressed in this manuscript are those of the authors and do not reflect the official views of the CARB. The authors would like to thank Dr. Gisele Olimpio da Rocha, Dr. Xiaobi M. Kuang,

Mr. David Gonzalez and Mr. J. Adlin Scott (UCLA) for their support in field measurement campaigns, Prof. Phil Rundel (UCLA) for help with species identification, and Mr. Faraz Enayati Ahangar, Mr. Seyedmorteza Amini and Prof. Akula Venkatram (U. California at Riverside) for sonic measurements and helpful discussions.

REFERENCES

Abhijith KV, Kumar P, Gallagher J, McNabola A, Baldauf R, Pilla F, et al. (2017). Air pollution abatement performances of green infrastructure in open road and built-up street canyon environments – A review. Atmospheric Environment, 162, 71–86. 10.1016/j.atmosenv.2017.05.014

Al-Dabbous AN, & Kumar P (2014). The influence of roadside vegetation barriers on airborne nanoparticles and pedestrians exposure under varying wind conditions. Atmospheric Environment, 90, 113–124. 10.1016/j.atmosenv.2014.03.040

Amini S, Ahangar FE, Schulte N, & Venkatram A (2016). Using models to interpret the impact of roadside barriers on near-road air quality. Atmospheric Environment, 138, 55–64. 10.1016/j.atmosenv.2016.05.001

Baldauf R, Thoma E, Khlystov A, Isakov V, Bowker G, Long T, & Snow R (2008). Impacts of noise barriers on near-road air quality. Atmospheric Environment, 42(32), 7502–7507. 10.1016/j.atmosenv.2008.05.051

Bowker GE, Baldauf R, Isakov V, Khlystov A, & Petersen W (2007). The effects of roadside structures on the transport and dispersion of ultrafine particles from highways. Atmospheric Environment, 41(37), 8128–8139. 10.1016/j.atmosenv.2007.06.064

Brantley HL, Hagler GSW, J. Deshmukh P, & Baldauf RW. (2014). Field assessment of the effects of roadside vegetation on near-road black carbon and particulate matter. Science of The Total Environment, 468–469, 120–129. 10.1016/j.scitotenv.2013.08.001

Chen L, Liu C, Zou R, Yang M, & Zhang Z (2016). Experimental examination of effectiveness of vegetation as bio-filter of particulate matters in the urban environment. Environmental Pollution, 208, 198–208. 10.1016/j.envpol.2015.09.006 [PubMed: 26385643]

Chen X, Pei T, Zhou Z, Teng M, He L, Luo M, & Liu X (2015). Efficiency differences of roadside greenbelts with three configurations in removing coarse particles (PM10): A street scale investigation in Wuhan, China. Urban Forestry & Urban Greening, 14(2), 354–360. 10.1016/j.ufug.2015.02.013

Choi W, & Paulson SE (2016). Closing the ultrafine particle number concentration budget at road-to-ambient scale: Implications for particle dynamics. Aerosol Science and Technology, 50(5), 448–461. 10.1080/02786826.2016.1155104

Choi W, He M, Barbesant V, Kozawa KH, Mara S, Winer AM, & Paulson SE (2012). Prevalence of wide area impacts downwind of freeways under pre-sunrise stable atmospheric conditions. Atmospheric Environment, 62, 318–327. 10.1016/j.atmosenv.2012.07.084

Choi W, Hu S, He M, Kozawa K, Mara S, Winer AM, & Paulson SE (2013). Neighborhood-scale air quality impacts of emissions from motor vehicles and aircraft. Atmospheric Environment, 80, 310–321. 10.1016/j.atmosenv.2013.07.043

Durant JL, Ash CA, Wood EC, Herndon SC, Jayne JT, Knighton WB, et al. (2010). Short-term variation in near-highway air pollutant gradients on a winter morning. Atmospheric Chemistry and Physics (Print), 10(2), 5599–5626.

Fantozzi F, Monaci F, Blanusa T, & Bargagli R (2015a). Spatio-temporal variations of ozone and nitrogen dioxide concentrations under urban trees and in a nearby open area. Urban Climate, 12(2), 119–127. 10.1016/j.uclim.2015.02.001

Fantozzi F, Monaci F, Blanusa T, & Bargagli R (2015b). Spatio-temporal variations of ozone and nitrogen dioxide concentrations under urban trees and in a nearby open area. Urban Climate, 12, 119–127. 10.1016/j.uclim.2015.02.001

Finn D, Clawson KL, Carter RG, Rich JD, Eckman RM, Perry SG, et al. (2010). Tracer studies to characterize the effects of roadside noise barriers on near-road pollutant dispersion under varying atmospheric stability conditions. Atmospheric Environment, 44(2), 204–214. 10.1016/j.atmosenv.2009.10.012

Fujii E, Lawton J, Cahill TA, Barnes DE, Hayes C, & Spada N (2008). Removal Rates of Particulate Matter onto Vegetation as a Function of Particle Size (Final Report to Breathe California of

Sacramento.). Breathe California of Sacramento-Emigrant Trails' Health Effects Task Force (HETF) and Sacramento Metropolitan Air Quality Management District.

Ghasemian M, Amini S, & Princevac M (2017). The influence of roadside solid and vegetation barriers on near-road air quality. Atmospheric Environment, 170, 108–117. 10.1016/j.atmosenv.2017.09.028

Gromke C, & Ruck B (2008). Aerodynamic modelling of trees for small-scale wind tunnel studies. Forestry: An International Journal of Forest Research, 81(3), 243–258. 10.1093/forestry/cpn027

Hagler GSW, Tang W, Freeman MJ, Heist DK, Perry SG, & Vette AF (2011). Model evaluation of roadside barrier impact on near-road air pollution. Atmospheric Environment, 45(15), 2522–2530. 10.1016/j.atmosenv.2011.02.030

Hagler GSW, Lin M-Y, Khlystov A, Baldauf RW, Isakov V, Faircloth J, & Jackson LE (2012). Field investigation of roadside vegetative and structural barrier impact on near-road ultrafine particle concentrations under a variety of wind conditions. Science of The Total Environment, 419, 7–15. 10.1016/j.scitotenv.2011.12.002 [PubMed: 22281040]

Health Effects Institute Panel on the Health Effects of Traffic-Related Air Pollution. (2010). Traffic-related air pollution: a critical review of the literature on emissions, exposure, and health effects. Health Effects Institute.

Heist DK, Perry SG, & Brixey LA (2009). A wind tunnel study of the effect of roadway configurations on the dispersion of traffic-related pollution. Atmospheric Environment, 43(32), 5101–5111. 10.1016/j.atmosenv.2009.06.034

Hölscher N, Höffer R, Niemann H-J, Brilon W, & Romberg E (1993). Wind tunnel experiments on micro-scale dispersion of exhausts from motorways. Science of The Total Environment, 134(1–3), 71–79. 10.1016/0048-9697(93)90340-C

Hu S, Fruin S, Kozawa K, Mara S, Paulson SE, & Winer AM (2009). A wide area of air pollutant impact downwind of a freeway during pre-sunrise hours. Atmospheric Environment, 43(16), 2541–2549. 10.1016/j.atmosenv.2009.02.033 [PubMed: 25379010]

Janhäll S (2015). Review on urban vegetation and particle air pollution – Deposition and dispersion. Atmospheric Environment, 105, 130–137. 10.1016/j.atmosenv.2015.01.052

Karner AA, Eisinger DS, & Niemeier DA (2010). Near-Roadway Air Quality: Synthesizing the Findings from Real-World Data. Environmental Science & Technology, 44(14), 5334–5344. 10.1021/es100008x [PubMed: 20560612]

Kent CW, Grimmond S, & Gatey D (2017). Aerodynamic roughness parameters in cities: Inclusion of vegetation. Journal of Wind Engineering and Industrial Aerodynamics, 169, 168–176. 10.1016/j.jweia.2017.07.016

Kumar P, Ketzel M, Vardoulakis S, Pirjola L, & Britter R (2011). Dynamics and dispersion modelling of nanoparticles from road traffic in the urban atmospheric environment—A review. Journal of Aerosol Science, 42(9), 580–603. 10.1016/j.jaerosci.2011.06.001

Lee ES, Ranasinghe DR, Ahangar FE, Amini S, Mara S, Choi W, et al. (2018). Field evaluation of vegetation and noise barriers for mitigation of near-freeway air pollution under variable wind conditions. Atmospheric Environment, 175, 92–99. 10.1016/j.atmosenv.2017.11.060

Lin M-Y, & Khlystov A (2012). Investigation of Ultrafine Particle Deposition to Vegetation Branches in a Wind Tunnel. Aerosol Science and Technology, 46(4), 465–472. 10.1080/02786826.2011.638346

Lin M-Y, Hagler G, Baldauf R, Isakov V, Lin H-Y, & Khlystov A (2016). The effects of vegetation barriers on near-road ultrafine particle number and carbon monoxide concentrations. Science of The Total Environment, 553, 372–379. 10.1016/j.scitotenv.2016.02.035 [PubMed: 26930311]

Morakinyo TE, Lam YF, & Hao S (2016). Evaluating the role of green infrastructures on near-road pollutant dispersion and removal: Modelling and measurement. Journal of Environmental Management, 182, 595–605. 10.1016/j.jenvman.2016.07.077 [PubMed: 27544646]

Ning Z, Hudda N, Daher N, Kam W, Herner J, Kozawa K, et al. (2010). Impact of roadside noise barriers on particle size distributions and pollutants concentrations near freeways. Atmospheric Environment, 44(26), 3118–3127. 10.1016/j.atmosenv.2010.05.033

Petroff A, Mailliat A, Amielh M, & Anselmet F (2008). Aerosol dry deposition on vegetative canopies. Part II: A new modelling approach and applications. Atmospheric Environment, 42(16), 3654–3683. 10.1016/j.atmosenv.2007.12.060

Ranasinghe DR, Choi W, Winer AM, & Paulson SE (2016). Developing High Spatial Resolution Concentration Maps Using Mobile Air Quality Measurements. Aerosol and Air Quality Research, 16(8), 1841–1853. 10.4209/aaqr.2015.07.0484

Steffens JT, Wang YJ, & Zhang KM (2012). Exploration of effects of a vegetation barrier on particle size distributions in a near-road environment. Atmospheric Environment, 50, 120–128.

Tong Z, Whitlow TH, MacRae PF, Landers AJ, & Harada Y (2015). Quantifying the effect of vegetation on near-road air quality using brief campaigns. Environmental Pollution, 201, 141–149. 10.1016/j.envpol.2015.02.026 [PubMed: 25797683]

Tiwary A, Morvan HP, & Colls JJ (2006). Modelling the size-dependent collection efficiency of hedgerows for ambient aerosols. Journal of Aerosol Science, 37(8), 990–1015. 10.1016/j.jaerosci.2005.07.004

Wang H, Takle ES, & Shen, and J (2001). SHELTERBELTS AND WINDBREAKS: Mathematical Modeling and Computer Simulations of Turbulent Flows. Annual Review of Fluid Mechanics, 33(1), 549–586. 10.1146/annurev.fluid.33.1.549

Fig. 1.

The mobile sampling route at the I-10 site in Santa Monica, CA (blue lines). The green lines denote the vegetation barriers and the red lines denote the sound walls. Map source: Google Earth.

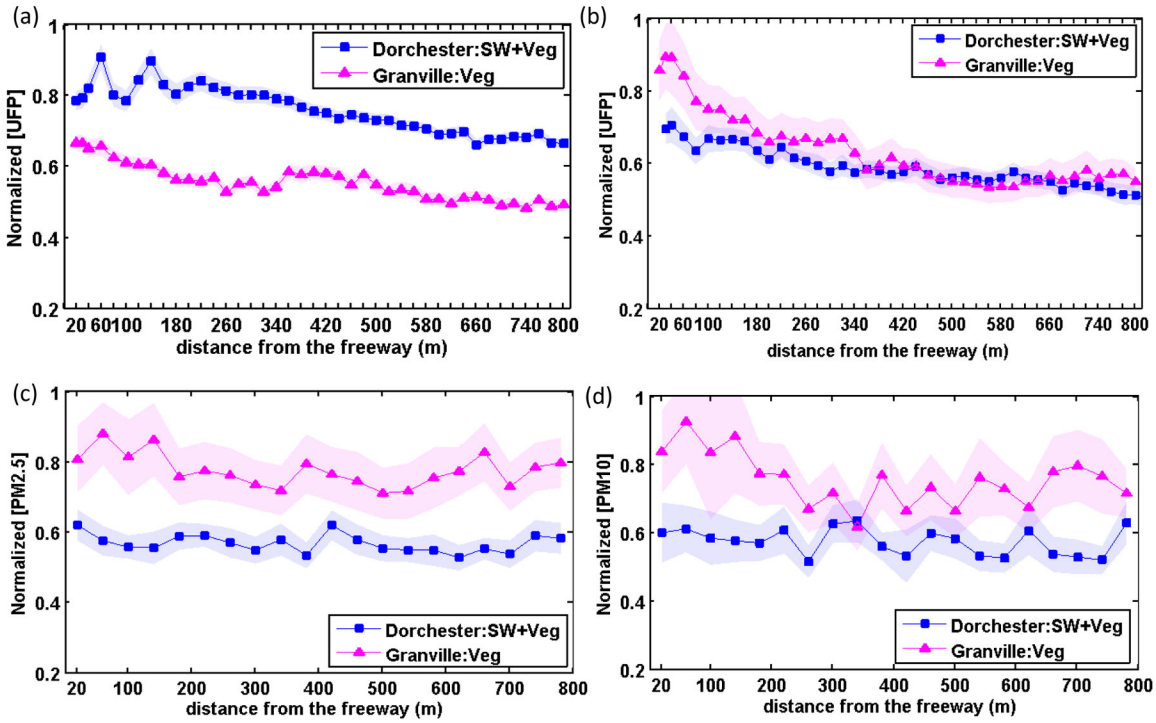

Fig. 2.

The normalized (a, b) UFP number concentration and (c) $PM_{2.5}$, (d) PM_{10} mass concentration along the two transects under perpendicular wind conditions for (a) summer-fall 2015 and (b, c, d) Winter 2016 measurement sessions. The traffic-normalized concentration averaged over (a) 8 and (b, c, d) 5 sessions (lines) is plotted together with the standard error of the mean (shaded areas).

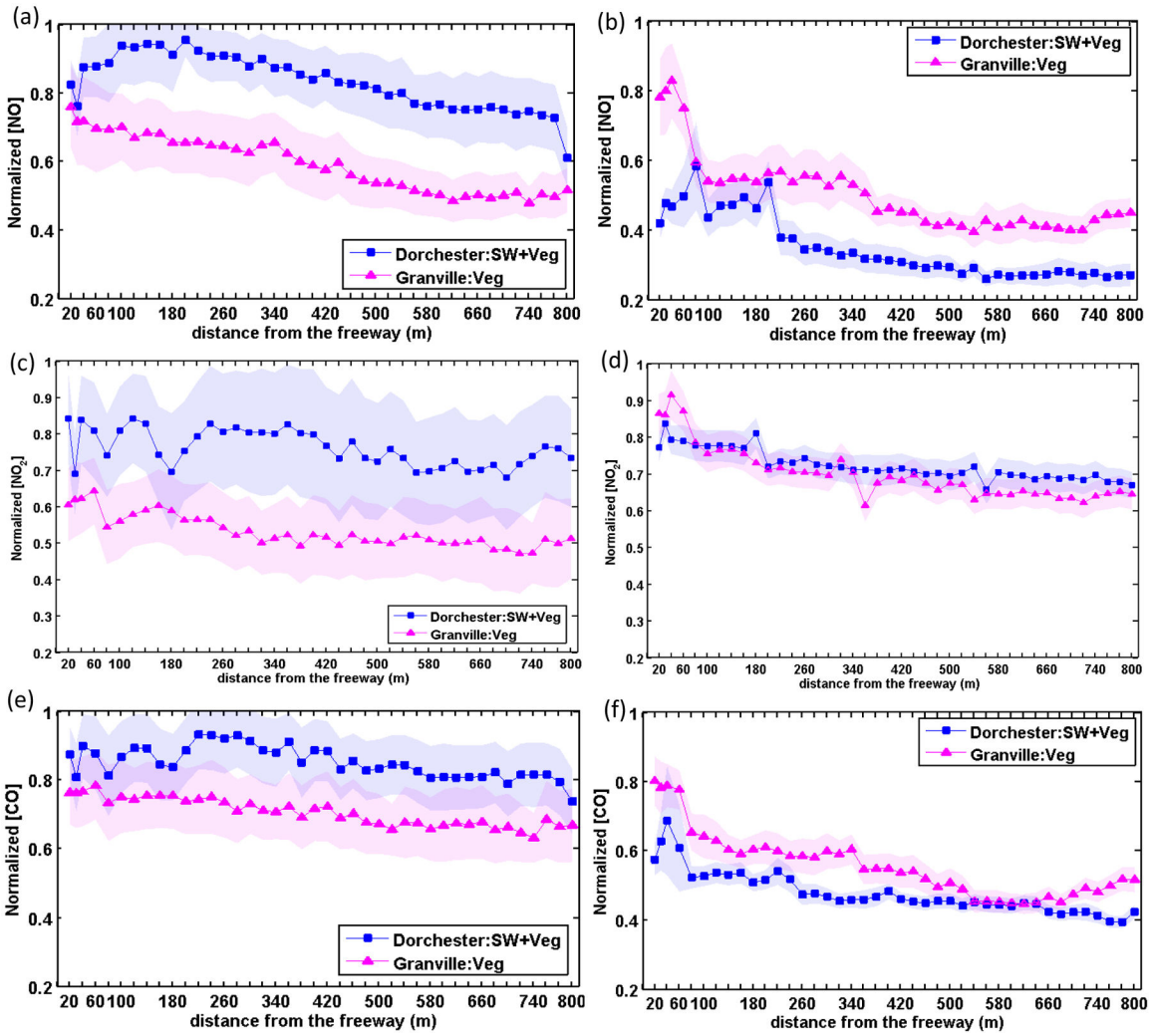

Fig. 3.

The normalized (a, b) NO, (c, d) NOx and (e, f) CO concentration along the two transects, under downwind conditions for (a, c, e) fall 2015 and (b, d, f) winter 2016 measurement sessions. The traffic-normalized concentration averaged over (a, c, e) 2 and (b, d, f) 5 sessions (lines) is plotted together with the standard error of the mean (shaded areas).

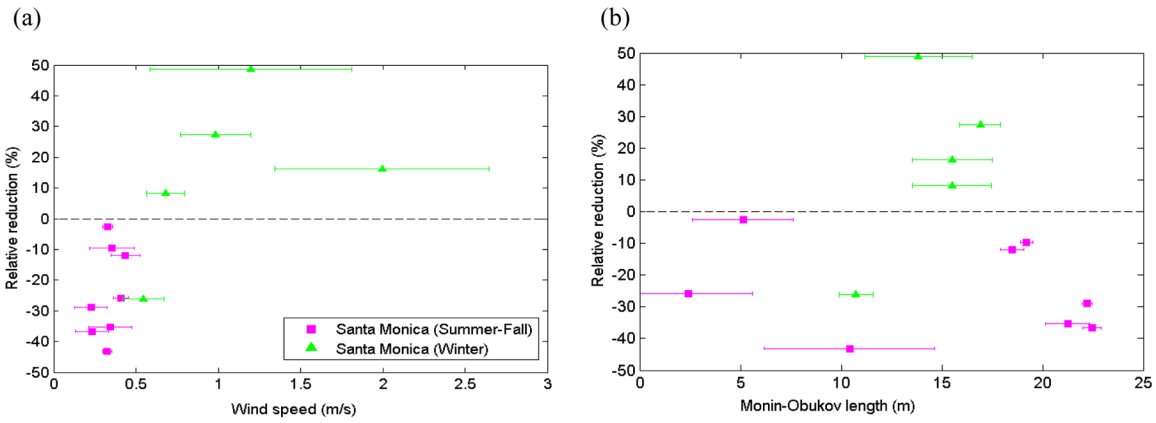

Fig. 4.

The relative [UFP] reduction by a combination barrier, under downwind conditions, averaged over the first 160 m from the edge of the freeway: VEG-CB/VEG as a function of the wind speed (a) and Monin-Obukov length (b). Session mean of meteorological parameters are plotted together with the standard error.

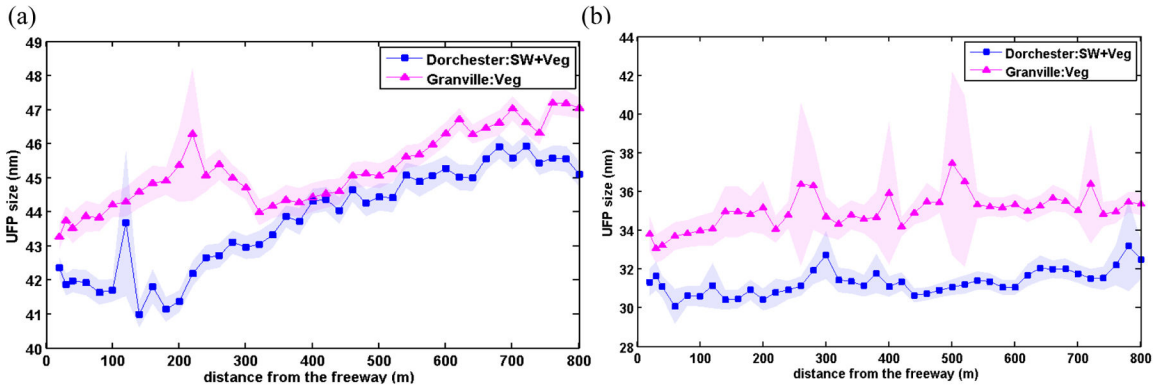

Fig. 5.

The mean diameter of UFP downwind of the barriers in the (a) summer-fall and (b) winter seasons, under downwind conditions. Session means (lines) are plotted together with the standard error (shaded area).

Table 1.

Monitoring instruments on the mobile monitoring platform used during fall and winter seasons

Instrument	Measurement Parameter	Response time[a] (Inlet to record)	Data time resolution
Testo DiSCmini	UFP count (10–700 nm), mean size	*2 s*	*1 s*
TSI OPS, Model 3330 *	Particle size (0.3–10 μm)	*3 s*	*5 s*
Teledyne API Model 300E	CO	*21 s*	*1 s*
LI-COR, Model LI-820	CO_2	*7 s*	*1 s*
Teledyne-API Model 200E	NO, NO_2, NO_x	*22 s*	*1 s*
Magee Scientific Aethalometer, AE-33 and AE-42	Black Carbon (BC)	*25 s*	*1 s*
Vaisala Sonic Anemometer and Temperature/ RH sensor	Surface winds, temperature, relative humidity (*RH*)	-	*1 s*
Qstar travel recorder XT[b]	GPS location	-	*1 s*
Eurotherm Chessell Graphic DAQ Recorder	Data-logger	-	*1 s*

[a]Response time is an averaged value for smoke test results and includes both the instrument response time and time to arrive from the inlet (Choi et al., 2013 (S3)).

[b]The GPS unit had 2.5 m accuracy when they are able to utilize wide area augmentation system (WAAS), a condition that applied during the measurements described here.

*Data not available during fall due to an instrument malfunction.

Table 2.

Measurement periods and surface meteorology at the sites

Date	Measurement Period	Mean wind speed (m/s)	Prevailing Wind direction[b]	Perpendicular wind percentage (%)[c]	Parallel wind percentage (%)[c]
Summer[a]					
08/12/15	05:15–07:00	0.44	NNW-NNE	81	14
08/13/15	05:00–06:45	0.35	NE-N	64	29
08/26/15	05:25–06:45	0.34	N	56	29
08/27/15	05:15–07:10	0.23	NNE-NNW	59	21
08/28/15	05:35–07:15	0.24	NNE-N	64	27
Fall					
10/01/15	05:40–07:30	0.33	NE	58	42
10/02/15	05:50–07:20	0.35	E-ENE	23	52
10/06/15	05:25–07:15	0.32	NE-ENE	8	75
10/08/15	05:50–07:40	0.33	N-NE	75	20
10/09/15	05:00–07:10	0.41	N-NE	59	30
Winter					
02/22/16	05:11–07:25	0.54	NE	50	44
02/24/16	04:52–07:12	0.98	NNE	74	26
02/25/16	05:04–07:47	0.68	NNE	70	30
03/08/16	05:26–07:35	2.00	NNW - NE	100	0
03/09/16	05:08–07:07	1.20	NE - N	49	39

[a] only UFP measurements

[b] prominent (>20% of the time) wind direction is noted first

[c] Mean of percentage of time each transect was under downwind/parallel wind condition (see text for definition) during full length of the measurement period

Table 3.

Relative reductions[a] (%) of pollutants

Site: Session	**calm (wind speed< 0.6 m/s)**		**light winds (0.6 m/s<wind speed< 3 m/s)**	
Pollutant	*Full*	*160 m*	*Full*	*160 m*
UFP	−24	−27	6	16
$PM_{2.5}$	−22[c]	1[c]	31	33
PM_{10}	−5[c]	40[c]	26	30
NO	−26	−16	29	26
NO2	−31	−21	2	6
CO	−21	−10	17	15

[a] relative reduction as defined in Section 4.2

[b] average of only positive values

[c] only one day

n/a- data not available

UFP-Ultrafine particles

PM-Particulate matter